DELPHI 97-70 CONF 56
28 July, 1997

Test of CP-violation in $e^+e^- \to Z \to \tau^+\tau^-$ and upper limit on the weak dipole moment of τ lepton

Preliminary

DELPHI Collaboration

M.-C. Chen, F. Grard and Ph. Herquet
Faculté des Sciences, Univ. de Mons-Hainaut

Abstract

Using the sample of $e^+e^- \to Z^0 \to \tau\bar{\tau}$ events accumulated at LEP with the DELPHI detector during 1992-1995, a direct test of CP-violation beyond the Standard Model is performed. From the events containing one- or three-prong τ decays, CP-odd optimised observables evaluated from the reconstructed τ momentum and polarisation vectors have been studied using τ decays into e, μ, π, ρ and a_1. No significant signal of CP-violation is observed, which leads to upper limits on the real and imaginary parts of the weak dipole form factor of the τ-lepton of $|\mathrm{Re}(d_\tau^w)| < 6.6 \times 10^{-18} e \cdot \mathrm{cm}$ and $|\mathrm{Im}(d_\tau^w)| < 2.0 \times 10^{-17} e \cdot \mathrm{cm}$.

Paper submitted to the LP'97 Conference
Hamburg, July 28 - August 1st

1 INTRODUCTION

CP-violation is a most promising direction in which to search for new physics beyond the Standard Model (SM). In the SM, CP-violation is described by a single phase in the three-generation quark mixing matrix, the Cabibbo-Kobayashi-Maskawa matrix [1]. Up to now, neutral kaon decays remain the only window to the observation of CP-violation. However the measured CP-violation parameter of the neutral K system, which fixes the value of the CP violating phase δ_{CKM} in the CKM matrix, does not test the SM assumption that δ_{CKM} constitutes the only source of CP-violation. Many procedures have been proposed to search for CP violating effects beyond the SM [2, 3]. One of them is to measure appropriate CP-odd observables, non-zero expectation values of which would provide direct evidence for CP violation beyond the SM [4]. As reviewed in [5], many measurements have been carried out accordingly at LEP1, where the channel $Z^0 \to \tau^+\tau^-$ is particularly promising and provides a high efficiency, low-background environment for such a search.

To the leading order in the electroweak interaction process $e^+e^- \to Z^0 \to \tau^+\tau^-$, a model-independent description of the CP violation is given by adding the following effective Lagrangian [4, 6] to the SM Lagrangian:

$$\mathcal{L}_{CP} \;=\; -\frac{1}{2}\, i\; \bar{\tau}\sigma^{\mu\nu}\gamma^5\tau[\; d_\tau^\gamma(q^2)F_{\mu\nu} \;+\; d_\tau^w(q^2)Z_{\mu\nu}\;] \tag{1}$$

where $F_{\mu\nu}$ and $Z_{\mu\nu}$ are the electromagnetic and weak field tensors of the SM. The new CP-violation effect arises from the interference between the SM amplitude and the CP-violating amplitude (1). The two form factors $d_\tau^\gamma(q^2)$ and $d_\tau^w(q^2)$ are referred to as the electric (EDM) and weak (WDM) dipole moment form factors respectively, and may have a real as well as imaginary parts. At the Z^0 resonance, the EDM $d_\tau^\gamma(M_Z^2)$ contribution appears as a radiative correction of $\mathcal{O}(\alpha)$ and can be neglected compared to the enhanced contribution of the WDM $d_\tau^w(M_Z^2)$ at the Z resonance.

The weak dipole moment of the τ lepton, $d_\tau^w(M_Z^2)$, can in principle be measured at LEP1 through the expectation values of appropriate CP-odd observables. Different observables have different sensitivities to CP-violating effects. In particular, a set of so-called optimised observables, $\mathcal{O}$, has been proposed [7] and used [8, 9, 10]. These optimised observables can be constructed from the τ momentum and its polarisation vectors, and can be expressed as follows:

$$\mathcal{O}^{Re} \;=\; \frac{1}{M_{SM}}(\hat{k}\cdot\hat{q}_e)(\hat{k}\times(S^+ - S^-))\cdot\hat{q}_e \tag{2}$$

$$\mathcal{O}^{Im} \;=\; \frac{1}{M_{SM}}(\hat{k}\cdot\hat{q}_e)[(\hat{k}\cdot S^+)(\hat{q}_e\cdot S^-) - (\hat{k}\cdot S^-)(\hat{q}_e\cdot S^+)] \tag{3}$$

$$\begin{aligned} M_{SM} \;=\; & 1 + (\hat{k}\cdot\hat{q}_e)^2 + S^+\cdot S^-(1-(\hat{k}\cdot\hat{q}_e)^2) - 2(\hat{q}_e\cdot S^+)(\hat{q}_e\cdot S^-) + \\ & 2(\hat{k}\cdot\hat{q}_e)[(\hat{k}\cdot S^+)(\hat{q}_e\cdot S^-) + (\hat{k}\cdot S^-)(\hat{q}_e\cdot S^+)] \end{aligned}$$

where the unit vector $\hat{k}$ is the momentum direction of the τ^+, $\hat{q}_e$ is the direction of the e^- beam, and the $S^\pm$ are the polarisation vectors of the $\tau^\pm$ in their respective rest systems. Neither $\hat{k}$ nor $S^\pm$ can be measured directly, they have to be reconstructed using the momenta of the τ-decay products (see Appendix).

The expectation values of the CP-odd observables can be calculated by integrating the differential cross-section for the process $e^+e^- \to Z^0 \to \tau^+\tau^-$ over the appropriate phase space, including the contribution from the SM as well as the additional effective CP-violating interaction (1). For small $d^w_\tau(M_Z)$, the expectation values of $\mathcal{O}^{Re}_{Im}$ are proportional to $\mathrm{Re}(d^w_\tau)$ and $\mathrm{Im}(d^w_\tau)$ respectively, i.e.,

$$
\begin{aligned}
< \mathcal{O}^{Re} >_{AB} &= \frac{M_Z}{e}\, c_{AB}\ \mathrm{Re}(d^w_\tau) \\
< \mathcal{O}^{Im} >_{AB} &= \frac{M_Z}{e}\, f_{AB}\ \mathrm{Im}(d^w_\tau)
\end{aligned}
\tag{4}
$$

where M_Z is the Z^0 mass and e is the electron charge. Here c_{AB} and f_{AB} are the decay channel ($\tau^+\tau^- \to A^+\bar{B}^-\nu_\tau\bar{\nu}_\tau$) dependent constants of proportionality, or sensitivities. These were calculated for each selected τ-pair decay channel used in the analysis by the Monte-Carlo method [11], taking into account the phase space cuts used for the selection of the τ-pair events. According to equation (4), CP violation introduced by $d^w_\tau(M_Z)$ can be measured through $< \mathcal{O}^{Re}_{Im} >$. Non-zero values would signal new physics of CP violation beyond the SM.

This letter presents a test of CP violation in $Z^0 \to \tau^+\tau^-$ using the optimised observables, based on the events accumulated by the DELPHI detector at the Z^0 peak during the 1992-1995 LEP1 runs. In section 2, the relevant detector components of DELPHI are briefly summarised. Section 3 describes the event selections. In section 4, the coefficients, c_{AB} and f_{AB}, are evaluated from a Monte Carlo simulation after the reconstruction of the τ momentum and the τ-spin vector. Systematic uncertainties are discussed in section 5, and the results are given in section 6.

2 THE DELPHI DETECTOR

The DELPHI detector and its performance are described in detail elsewhere [12, 13]. The sub-detector units particularly relevant for this analysis are summarised here. In the DELPHI reference frame the z-axis is taken along the direction of the e^- beam. The angle θ is the polar angle defined with respect to the z-axis and ϕ is the azimuthal angle about this axis. The reconstruction of a charged particle trajectory in the barrel ($|\cos\theta| < 0.732$) and forward ($0.732 < |\cos\theta| < 0.94$) regions of DELPHI resulted from a combination of the measurements in:

- the Vertex Detector (VD), made of three layers of single-sided silicon microstrip modules, with an angular coverage of $25° \leq \theta \leq 155°$, a space point resolution in $r\phi$ of about 8 μm, and a two track separation of 100 μm.

- the Inner Detector (ID), a jet chamber measured $r\phi$ coordinates and provided track reconstruction, in the angular range $15° \leq \theta \leq 165°$. Its two track separation in $r\phi$ was 1 mm and its spatial resolution 50 μm.

- the Time Projection Chamber (TPC), the main detector for the track reconstruction, which provided up to 16 space points for pattern recognition, and ionization information (dE/dx) extracted from the wires. It had an angular coverage of $20° \leq \theta \leq 160°$ and a two track separation of about 1.5 cm in $r\phi$ and in z.

- the Outer Detector (OD), five layers of drift tubes covering the angular range of $42° \leq \theta \leq 138°$ Each layer provided a space point with 110 μm precision in $r\phi$.

- the Forward Chambers A (FCA), made of three modules each of which consists of two staggered planes of drift tubes. This chamber covers polar angles of $11° \leq \theta \leq 32°$ and $148° \leq \theta \leq 169°$. For reconstructed track elements, it has precisions of $\sigma_x = 290\ \mu$m, $\sigma_y = 240\ \mu$m, $\sigma_\theta = 8.5$ mrad and σ_ϕ averaged over θ is 24 mrad.

- the Forward Chambers B (FCB), drift chambers covering polar angles of $11° \leq \theta \leq 36°$ and $144° \leq \theta \leq 169°$. The precision achieved on the parameters of the reconstructed track elements are $\sigma_{x,y} = 150\ \mu$m, $\sigma_\theta = 3.5$ mrad and $\sigma_\phi = 4.0/\sin\theta$ mrad.

These detectors were surrounded by a solenoidal magnet with a 1.2 Tesla field parallel to the z-axis. In addition to the detectors mentioned above, the identification of the τ decay products relied on:

- the barrel electromagnetic calorimeter (HPC), a High density Projection Chamber with eighteen radiation lengths deep for perpendicular incidence and polar angle coverage of $43° \leq \theta \leq 143°$. Its energy resolution was $\Delta E/E = 6.5\%$ for electrons with a energy of 45.6 GeV.

- the forward electromagnetic calorimeter (FEMC), consisting of two arrays of Cherenkov lead glass blocks, covering the polar angles $8° \leq \theta \leq 35°$ and $145° \leq \theta \leq 172°$. The energy resolution for 45.6 GeV electrons is 4.8%.

- the Hadron Calorimeter (HCAL), segmented in 4 layers in depth, with a granularity of 3.75° in polar and 2.96° in azimuthal angle. It covers almost the full solid angle: $11° \leq \theta \leq 169°$.

- the barrel, forward and surrounding Muon Chambers (MUB, MUF and SMU), the MUB and MUF consisting of two layers of drift tubes and the SMU of a single layer filling the gap in θ between MUB and MUF. Together they cover the polar angle region of $20° \leq \theta \leq 160°$.

3 EVENT SELECTION

The events were selected in two steps. Firstly, $Z^0 \to \tau^+\tau^-$ events were selected from a high purity sample of dilepton events ($e^+e^- \to e^+e^-$, $\mu^+\mu^-$, $\tau^+\tau^-$) from which cosmic rays, $e^+e^- \to q\bar{q}$ events, and two photon $e^+e^- \to (e^+e^-)X$ events were removed. In the second step, specific τ-decay modes including $\tau \to e\nu_\tau\bar{\nu}_e$, $\mu\nu_\tau\bar{\nu}_\mu$, $\pi(K)\nu_\tau$, $\rho\nu_\tau$ and $a_1\nu_\tau \to \pi^\pm\pi^\pm\pi^\mp\nu_\tau$ were selected from this sample.

3.1 τ-pair selection

Around the Z^0 resonance, a $\tau^+\tau^-$ event appears as two highly collimated low multiplicity jets emerging in opposite directions. It is divided into hemispheres by a plane perpendicular to the event thrust axis, which is determined using all charged particles. The accepted event topology contains one or three charged particles in each hemisphere, lying in the polar angle region $|\cos\theta| < 0.94$.

Cosmic rays were rejected by requiring the charged particles in each hemisphere to have a distance of closest approach to the interaction region less than 4.5 cm in z and less than 1.5 cm in the $r\phi$ plane. The off-set in z of tracks in opposite hemispheres of the TPC being sensitive to the time of passage of a cosmic ray with respect to the time of interaction of the beams, the particles were also required to have a difference in z of their points of closest approach at the interaction region of less than 3 cm.

Two photon events were rejected by requiring a total energy in the event greater than 8 GeV and a total event transverse momentum greater than 0.4 GeV/c. The residual background from $e^+e^- \to q\bar{q}$ was reduced by requiring a charge particle multiplicity less than six and an isolation angle, defined as the minimum angle between any two charged particles in opposite hemispheres, greater than 160°.

The presence of $e^+e^- \to e^+e^-$ and $e^+e^- \to \mu^+\mu^-$ events was reduced by requiring the acollinearity angle between the two tracks to be less than 0.5°, the radial momentum $P_{rad} = (p_1^2 + p_2^2)^{1/2}$ to be less than the beam momentum , and the radial energy $E_{rad} = (E_1^2 + E_2^2)^{1/2}$ be less than the beam energy. The variables E_1 and E_2 are the total electromagnetic energy deposited in cones of half angle 30° about the particle momenta p_1 and p_2 respectively.

For determining the efficiency of the selection of events and for estimating the backgrounds, simulated event samples have been used which had been passed through a detailed simulation of the detector response [13] and reconstructed and analysed with the same programs as the real data. Various Monte Carlo event generators were used: KORALZ [14] for $e^+e^- \to \tau^+\tau^-$ events; DYMU3 [15] for $e^+e^- \to \mu^+\mu^-$ events; BABAMC [16] for $e^+e^- \to e^+e^-$ events; JETSET [17] for $e^+e^- \to q\bar{q}$ events; Berends-Davereldt-Kleiss [18] for $e^+e^- \to (e^+e^-)e^+e^-$ events; and the generator described in [19] for $e^+e^- \to (e^+e^-)\mu^+\mu^-$ and $e^+e^- \to (e^+e^-)\tau^+\tau^-$ events.

In total, 141340 τ-pair candidate events were selected in the polar angle region $|\cos\theta| < 0.94$, with a total background of 3.5% estimated from the simulated data sample: 1.24% from $e^+e^- \to e^+e^-$; 0.47% from $e^+e^- \to \mu^+\mu^-$; 0.7% from $e^+e^- \to q\bar{q}$; and 1.16% from other non-τ events.

3.2 τ-decay selection

The selection criteria used for the identification of τ decays in the DELPHI barrel region are described in detail in [20]. In this analysis, the angular acceptances were extended to the forward region of DELPHI detector: $0.804 < |\cos\theta| < 0.940$ for electrons and pions; $0.732 < |\cos\theta| < 0.940$ for muons and the a_1. The selection criteria were similar in the forward and barrel regions, and are briefly summarised as follows.

The electron identification is based on the ionisation loss (dE/dx) in the TPC and the energy deposited in the forward electromagnetic calorimeter (FEMC). Two pull variables are used to separate electrons from muons and hadrons, defined as the differences between the measured variables dE/dx and E_{ass}/p and their expected values for electrons, divided by their measurement errors (Fig.1a and 1b).

The muon identification is based on requiring a reasonably uniform energy deposition in the four layers of the hadronic calorimeter (HCAL) compatible with that expected for a minimum ionising particle (Fig.1c), a signal in the muon chambers, and a low energy deposition in the electromagnetic calorimeter.

A charged pion is identified by requiring low energy deposition in the electromagnetic calorimeter where the hadronic interaction probability is small, hadronic deposition in the HCAL, no signal in the muon chambers, and a dE/dx measurement compatible with that expected for a pion (with a pull variable as defined above, see Fig.1d).

A photon is defined as a shower in the electromagnetic calorimeter not associated to a track and fulfilling quality cuts on minimum energy and shower profile.

A π^0 is reconstructed as two photons with an invariant mass compatible with a π^0 (Fig.2a), or as a single unresolved energetic shower in the electromagnetic calorimeter.

A ρ is defined as a single pion with an accompanying π^0 and with a total invariant mass compatible with the ρ mass (Fig.2b).

An a_1 is recognised as three pions without any π^0 and with a total invariant mass compatible with the a_1 mass (Fig.2c).

The selection efficiencies and purities, after the rejection of background events, are summarised in Table 1 for all the τ decay channels used in the analysis. In total, 21641 events were selected in the 9 different τ-pair decay channels listed in Table 2.

4 Proportionality Coefficients: c_{AB} and f_{AB}

The coefficients in equation (4) can be calculated by numerical integration over the appropriate phase space for the corresponding observables $\mathcal{O}^{Re}_{Im}$ which are reconstructed from the τ momenta and spin vectors. Neither the τ momenta nor their spin directions can be measured directly, due to the undetected neutrinos from the τ decays.

It is well known [21] that, in the case of two-body τ decays, the τ momenta can be reconstructed up to a two-fold ambiguity, assuming the $\tau^+\tau^-$ pair is produced in a back-to-back topology. The existence of this ambiguity would in turn reduce the analysing power of the CP-odd observables, $\mathcal{O}^{Re}_{Im}$, to the measurement of CP-violation. This can in principle be improved by resolving the ambiguity using a microvertex detector to measure the impact parameters near the interaction region [21]. However this resolution is not absolutely necessary as compared with the dominant statistical errors of the measurement [9]. In the present analysis, the τ flight direction was reconstructed by averaging over the two possible solutions, i.e. neglecting the ambiguities (see Appendix). For the events including leptonic τ decays, the reconstruction of the τ flight direction gives only approximate results.

The τ-spin, i.e. its polarisation vector, can be estimated in the τ rest frame from the resultant momentum of its decay products, by taking advantage of the fact that the parity violation in τ decay makes the τ-decay products τ-spin analysers [22]. The partial decay width for the channel $\tau \to A(\hat{p}_A) + X$, where X stands for neutral hadrons or neutrinos, can be expressed as [22, 6]

$$d\Gamma \propto (1 + \alpha_A \hat{p}_A \cdot S_\tau) \cdot \frac{d\Omega}{4\pi} \qquad (5)$$

where $\hat{p}_A$ is the momentum direction of charged particle A in the τ rest frame, S_τ is the τ-spin vector, and α_A is a measure of the spin-analysing power of the decay channel. It is well known that the decay channel $\tau \to \pi\nu_\tau$ provides the best spin-analyser, as the parameter $\alpha_{\pi\nu}$ takes its maximal value $\alpha_{\pi\nu} = 1$. For a given τ decay channel, the best estimator of the τ-spin direction is that for which (5) is maximal.

The τ-spin vectors constructed from the 4-momenta of the τ decay products for various channels have been calculated in [7] and are listed in the Appendix. Due to the limited detector resolution and the existence of ambiguity in the reconstructed τ direction, the reconstructed τ-spin vectors are spread and reduced from their theoretical magnitudes, as shown in Fig. 3.

Using the reconstructed τ-flight and τ-spin vectors, the coefficients c_{AB} and f_{AB} were calculated for simulated events in the same geometric and momentum acceptance as for the real data, using a Monte Carlo program which includes CP-violation according to equation (1) in addition to the SM Lagrangian.

5 Systematic Uncertainties

Various sources of systematic uncertainties which might affect the determination of the coefficients c_{AB} and f_{AB} and the expectation value of the CP-odd observables were studied for each selected τ decay channel.

The contamination of other τ decays in a selected τ-pair decay channel reduces the analysing power of that channel, since the observables were not optimised for these background events. These effects were taken into account by averaging the coefficients c_{AB} and f_{AB} over all of the components contributing to selected channel with the corresponding composition fractions as the weights, i.e. $c_{AB}^{eff} = \Sigma n_{ab}c_{ab}/\Sigma n_{ab}$. This leads to effective values of the coefficients c_{AB}^{eff} and f_{AB}^{eff}, which in general are smaller than the corresponding values without contamination. Backgrounds from other τ decays (e.g. $\tau \to 3\pi n\pi^0$) and from non-τ events (e.g. $e^+e^- \to e^+e^-$, $e^+e^- \to \mu^+\mu^-$ and $e^+e^- \to q\bar{q}$) were assumed to be CP symmetric.

The contributions to the systematic error coming from the finite Monte Carlo statistics in the calculation of c_{AB} and f_{AB} and in the determination of background were estimated by taking the corresponding errors at one standard deviation level.

Table 2 gives the values of the coefficients c_{AB}^{eff} and f_{AB}^{eff} for the forward and barrel region, and the numbers of selected events.

An important source of systematic error in determining the expectation values of the CP-odd observables is the possible CP-asymmetry of the detector, which could fake a CP-violation effect. A generic check of this possibility was made by constructing, from the selected data sample, a reference data sample in which the spin-correlation between the τ^+ and τ^- was destroyed; this was done by mixing a τ decay from one τ-pair event with one having the opposite charge and angular orientation (within 1°) taken from another τ-pair event. Monte Carlo study confirmed a complete destruction of the spin-correlation after this mixing; what remains in the reference data sample is only the detector effects. The errors within which a zero expectation value could be extracted from the reference data sample were taken as the uncertainty from the CP-asymmetry of the detector and from the cuts for event selection. They vary from 18% ($\tau^+\tau^- \to ll\nu_l\bar{\nu}_l\nu_\tau\bar{\nu}_\tau$) to 5% ($\tau^+\tau^- \to \rho\pi\nu_\tau\bar{\nu}_\tau$) of the corresponding statistical errors for the τ-pair decay channels.

All the systematic errors considered were determined for each τ-pair decay channel and propagated to the calculation of $\mathrm{Re}(d_\tau^w)$ and $\mathrm{Im}(d_\tau^w)$.

6 Results and Conclusion

For the test of CP-violation with the optimised observables, the mean values of the distributions of the measured $\mathcal{O}_{Im}^{Re}$ show no significant deviation from zero (Fig.4). Thus the results of this analysis show no signal of CP-violation effects.

Using the effective coefficients c_{AB}^{eff} and f_{AB}^{eff}, the value of the weak dipole moments, $\mathrm{Re}(d_\tau^w)$ and $\mathrm{Im}(d_\tau^w)$, are deduced from the measured $< \mathcal{O}_{Im}^{Re} >$ as shown in Fig.5, where their magnitudes are again seen to be compatible with zero for all the τ-pair decay channels investigated.

Combining the results from all channels for the 92-95 data, one obtains:

$$\mathrm{Re}(d_\tau^w) = (-1.48 \pm 2.64_{stat} \pm 0.27_{sys}) \times 10^{-18} e \cdot \mathrm{cm}$$
$$\mathrm{Im}(d_\tau^w) = (-0.44 \pm 0.77_{stat} \pm 0.13_{sys}) \times 10^{-17} e \cdot \mathrm{cm}$$

This null measurement leads to upper limits on the real and imaginary part of the weak dipole moment d_τ^w:

$$|\mathrm{Re}(d_\tau^w)| < 6.6 \times 10^{-18} e \cdot \mathrm{cm}$$
$$|\mathrm{Im}(d_\tau^w)| < 2.0 \times 10^{-17} e \cdot \mathrm{cm}$$

at 95% confidence level.

Acknowledgements

We are greatly indebted to our technical collaborators and to the agencies for their support in building and operating the DELPHI detector, and to the members of the CERN-SL Division for the excellent performance of the LEP collider. We also would like to express our gratitude to Dr. P. Overmann for numerous helpful discussions and for the Monte Carlo program to calculate the coefficients according to equation (1).

Appendix: Reconstruction of τ-momentum and polarisation

In the process $e^+e^- \to \tau^+(k^+)\tau^-(k^-) \to A^+(p_A)\bar{B}^-(p_B)\nu_\tau\bar{\nu}_\tau$, the τ momentum can be reconstructed up to a two-fold ambiguity if the momenta of all final state hadrons are known and simple two-body kinematics is assumed. Neglecting the ambiguity, which is only of the order of $m_\tau/|k|$, the τ^+ momentum k can be reconstructed as:

$$k \approx u\hat{p}_A + v\hat{p}_B.$$

$$u = \frac{\alpha_A + \hat{p}_A \cdot \hat{p}_B \alpha_B}{1 - (\hat{p}_A \cdot \hat{p}_B)^2}, \qquad v = -\frac{\alpha_B + \hat{p}_A \cdot \hat{p}_B \alpha_A}{1 - (\hat{p}_A \cdot \hat{p}_B)^2}.$$

where hats denote unit momenta, and

$$\alpha_i = \frac{\sqrt{s} E_i - m_\tau^2 - m_i^2}{2|p_i|} \qquad (i = A, B)$$

where $(E_i,\, p_i)$ are the resultant 4-momenta of the observed τ decay products, m_i their invariant mass, and s the centre-of-mass energy.

The τ polarisation vectors can be taken as the expectation values of the momentum of the charged decay products in the τ rest frame, and can be expressed for different channels as [7]:

$$[S^\pm]_{\tau\to\pi\nu} = \frac{2}{m_\tau^2 - m_i^2}(\mp m_\tau p_\pi + \frac{m_\tau^2 + m_i^2 + 2m_\tau E_{\pi^\pm}}{2(k_0 + m_\tau)} k)$$

$$[S^\pm]_{\tau\to\rho\nu\to\pi\pi^0\nu} = \mp \frac{\mp H_0^\pm k + m_\tau H^\pm + k(k \cdot H^\pm)/(k + m_\tau)}{(k^\pm H^\pm) - m_\tau^2 (p_{\pi^\pm} - p_{\pi^0})^2}$$

where the components of the 4-vector $H^\pm$ are $(H^\pm)^\nu = 2(p_{\pi^\pm} - p_{\pi^0})^\nu (p_{\pi^\pm} - p_{\pi^0})^\mu (k_\pm)_\mu + (p_{\pi^\pm} + p_{\pi^0})^\nu (p_{\pi^\pm} - p_{\pi^0})^2$,

$$[S^\pm]_{\tau\to l\nu\bar{\nu}} = \frac{4c^\pm - m_\tau^2}{3m_\tau^2 c^\pm - 4c_\pm^2}(\mp m_\tau p^\pm - k\frac{c^\pm + E^\pm m_\tau}{k_0 + m_\tau})$$

where $c^\pm = k_0 E^\pm \mp k \cdot p^\pm$. In these formulae, k stands for the real τ-momentum, but in the analysis it was replaced by the reconstructed one.

For $\tau \to a_1\nu \to \rho\pi\nu$ the notation is

$$\tau(t) \to \nu + \pi(p) + \rho(r)$$

where $t = (t_0, \vec{t})$, $p = (p_0, \vec{p})$ and $r = (r_0, \vec{r})$. The spin-vector in this case is

$$[S^\pm]_{\tau\to a_1\nu\to\rho\pi\nu} = \pm \frac{\frac{\vec{t}}{t_0 + m_\tau}(vt) + v_0 m_\tau - m_\tau \vec{v}}{vt + m_\tau^2 (ar)^2}$$

where the four-vector v is defined as

$$v^\mu = a^\mu[(ar)^2(2at/a^2 - 1) + 2r^2(at - a^2) - 2(ar)(tr)] + r^\mu[2a^2(rt) - 2(ar)(at)]$$

with $a = r + p$.

References

[1] M. Kobayashi and T. Maskawa, Prog. Theor. Phys. **49** (1973) 652.

[2] Y. Grossman, Y. Nir, R. Rattazzi, CERN-TH/96-368.

[3] W. Bernreuther, Talk given at the 20th Johns Hopkins Workshop, Heideberg, June 1996, PITHA 97/3.

[4] W. Bernreuther, U. Löw, J.P. Ma and O. Nachtmann, Z. Phys. **C43** (1989) 117;
W. Bernreuther, O. Nachtmann, Phys. Rev. Lett. **63** (1989) 2787;
W. Bernreuther, G.W. Botz, O. Nachtmann and P. Overmann, Z. Phys. **C52** (1991) 567;
W. Bernreuther, O. Nachtmann and P. Overmann, Phys. Rev. **D48** (1993) 78;
W. Bernreuther, O. Nachtmann, Z. Phys. **C73** (1997) 647;
W. Bernreuther, A. Brandenburg and P. Overmann, Phys. Lett. **B391** (1997) 413.

[5] N. Wermes, Invited talk at 4th International Workshop on Tau Lepton Physics (TAU 96), Estes Park, Colorado, 16-19 Sep 1996, http://tau96.colorado.edu/tau96/ps/-wermes.ps, Bonn preprint BONN-HE-96-10 (1996).

[6] W. Bernreuther, O. Nachtmann and P. Overmann, Phys. Rev. **D48** (1993) 78.

[7] P. Overmann, *A new method to measure the τ polarisation at the Z peak*, Univ. of Dortmund: DO-TH 93/24.

[8] ALEPH Coll., D. Buskulic et al., Phys. Lett. **B346** (1995) 371.

[9] OPAL Coll., R. Akers et al., Z. Phys. **C66** (1995) 31.

[10] OPAL Coll., K. Ackerstaff et al., Z. Phys. **C74** (1997) 403

[11] P. Overmann, Univ. of Heidelberg: *TAUMC*, private communication.

[12] DELPHI Coll., P. Aarnio et al., Nucl. Instr. and Meth. **A303** (1991) 233.

[13] DELPHI Coll., P. Abreu et al., Nucl. Instr. and Meth. **A378** (1996) 57.

[14] S. Jadach and Z. Was, Comp. Phys. Comm. **36** (1985) 191;
S. Jadach, B.F.L. Ward and Z. Was, Comp. Phys. Comm. **66** (1991) 276.

[15] J.E. Campagne and R. Zitoun, Z. Phys. **C43** (1989) 469.

[16] F.A. Berends, W. Hollik and R. Kleiss, Nucl. Phys. **B304** (1988) 712.

[17] T. Sjöstrand, Comp. Phys. Comm. **27** (1982) 243, ibid. **28** (1983) 229;
T. Sjöstrand and M. Bengtsson, Comp. Phys. Comm. **43** (1987) 367;
T. Sjöstrand, *PYTHIA 5.6 JETSET 7.3 Physics and manual*, CERN-TH 6488/92 (1992).

[18] F.A. Berends, P.H. Daverveldt and R. Kleiss, Phys. Lett. **B148** (1984) 489;
Comp. Phys. Comm. **40** (1986) 271.

[19] T. Todorov, *Détermination des paramètres du modèle standard et teste de sa validité dans les désintegrations hadroniques du Z^0*, Doctoral Thesis, CRN Strasbourg, report CRN/HE 94-21, 1994.

[20] DELPHI Coll., P. Abreu et al., Z. Phys. **C67** (1995) 183.

[21] J.H. Kühn, Phys. lett. **B313** (1993) 458.

[22] Y.S. Tsai, Phys. Rev., **D4** (1971) 2821.

Selected τ-decay channel	selection efficiency	Composition (%)					others
		e	μ	π	ρ	a_1	
e	82.6	95.0	0.0	0.9	2.7	1.0	0.4
μ	84.2	0.0	99.0	0.7	0.3	0.0	0.0
π	60.7	0.6	4.7	86.3	5.2	0.1	3.2
ρ	57.0	0.1	0.2	5.7	74.1	13.8	6.1
a_1	55.1	0.0	0.0	0.0	0.5	90.0	9.5

Table 1: The overall selection efficiencies and purities of the τ decay channels selected in the 92-95 data, as determined from the simulation. The angular acceptance is $|\cos\theta| < 0.94$.

Selected $\tau\bar{\tau}$-decay channel	Barrel			Forward		
	Number of Events	c_{AB}^{eff}	f_{AB}^{eff}	*Number of Events*	c_{AB}^{eff}	f_{AB}^{eff}
$\pi\pi$	274	0.227±0.032	-0.047±0.006	38	0.122±0.005	-0.039±0.002
$l\ l$	5368	0.047±0.002	-0.003±0.001	1429	0.041±0.002	-0.006±0.001
$\rho\rho$	1201	0.185±0.016	-0.042±0.003	78	0.138±0.012	-0.039±0.004
$\pi\ l$	2505	0.127±0.007	-0.013±0.001	524	0.078±0.003	-0.016±0.001
$\rho\pi$	1097	0.202±0.017	-0.046±0.003	125	0.122±0.004	-0.037±0.001
$\rho\ l$	5120	0.119±0.007	-0.015±0.001	640	0.085±0.002	-0.016±0.001
$a_1 l$	1680	0.043±0.007	-0.006±0.001	313	0.043±0.003	-0.003±0.001
$a_1\rho$	768	0.093±0.011	-0.008±0.001	53	0.086±0.008	-0.009±0.001
$a_1\pi$	384	0.099±0.013	-0.008±0.001	44	0.064±0.006	-0.009±0.001

Table 2: The effective values of the coefficients of proportionality for each τ-pair decay channel, determined from the simulation and used to calculate the weak dipole moment d_τ^w from the measured expectation values of the optimised observables for the selected events.

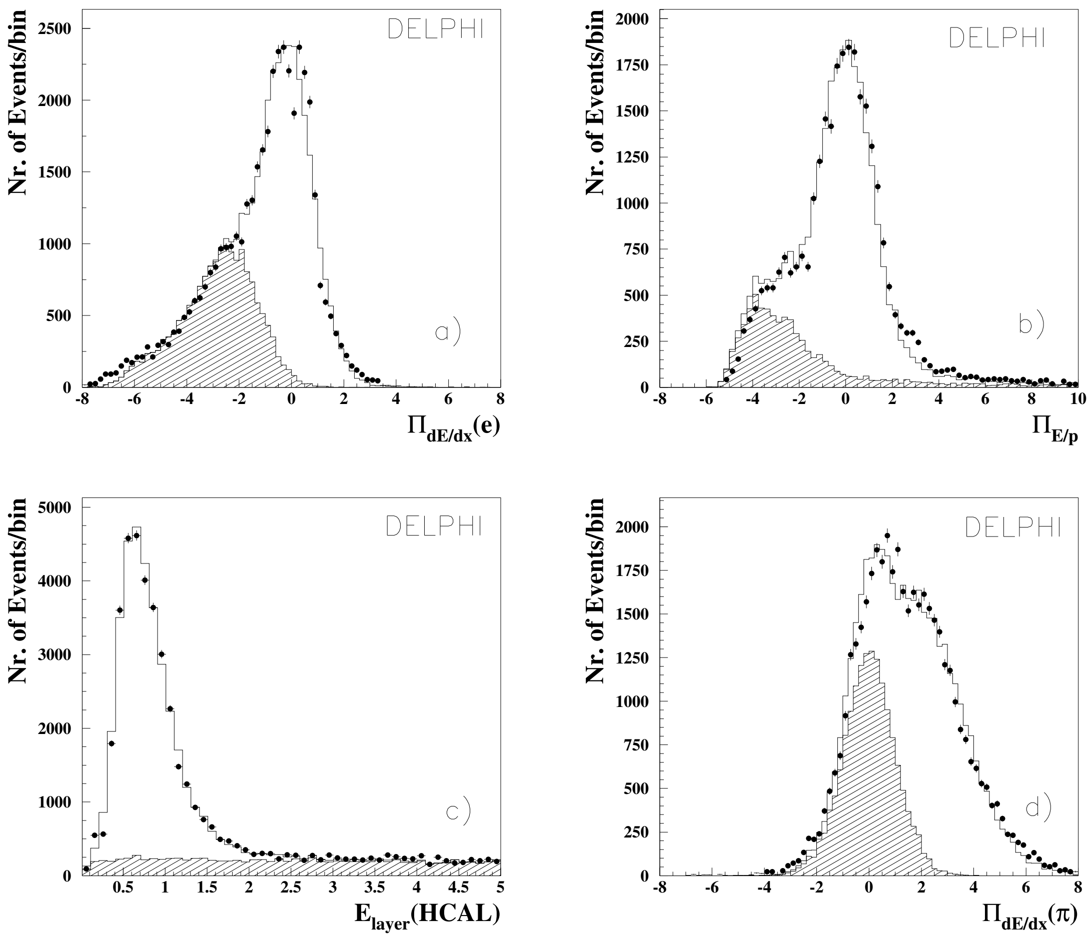

Figure 1: Distribution of the pull variables used for τ-decay identification (hereafter all the figures represent the data in the angular acceptance $|\cos\theta| < 0.94$). The clear parts of the histograms show the corresponding simulated signals for a) and b) $\tau \to e\nu\bar{\nu}$ decay, c) $\tau \to \mu\nu\bar{\nu}$ decay, and d) $\tau \to \pi\bar{\nu}$ decay; the hatched parts show the corresponding backgrounds; and the dots with error bars show the data.

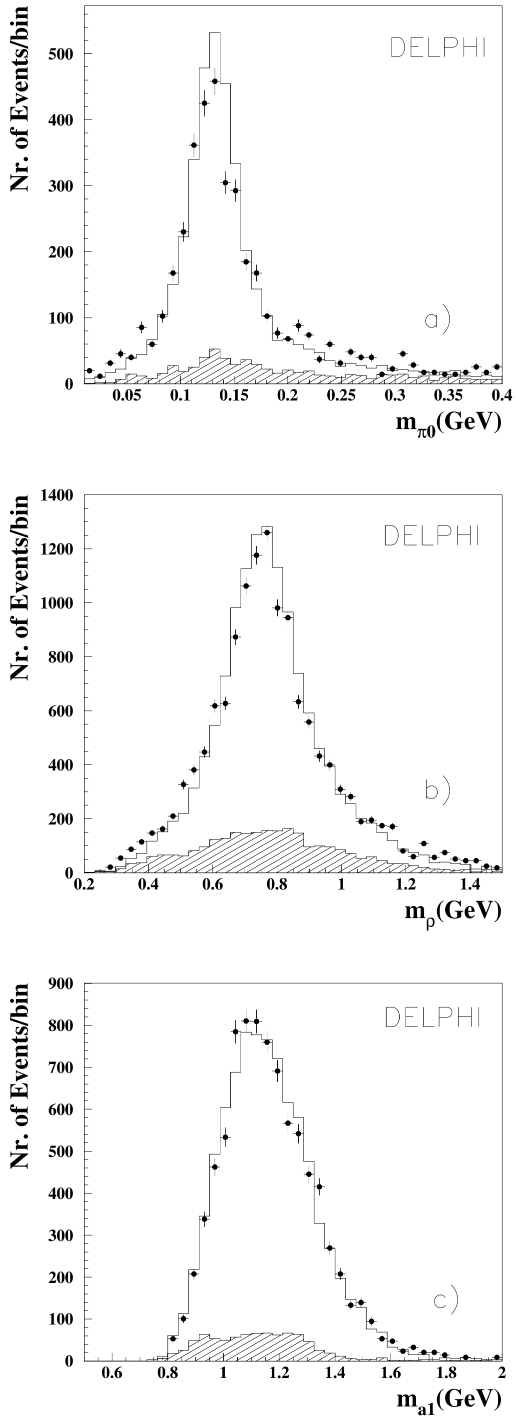

Figure 2: Distribution of the reconstructed invariant mass of: $a)$ π^0; $b)$ ρ; and $c)$ a_1. The dots with error bars show the data; the clear parts of the histograms show the simulated data; and the hatched parts show the background contribution.

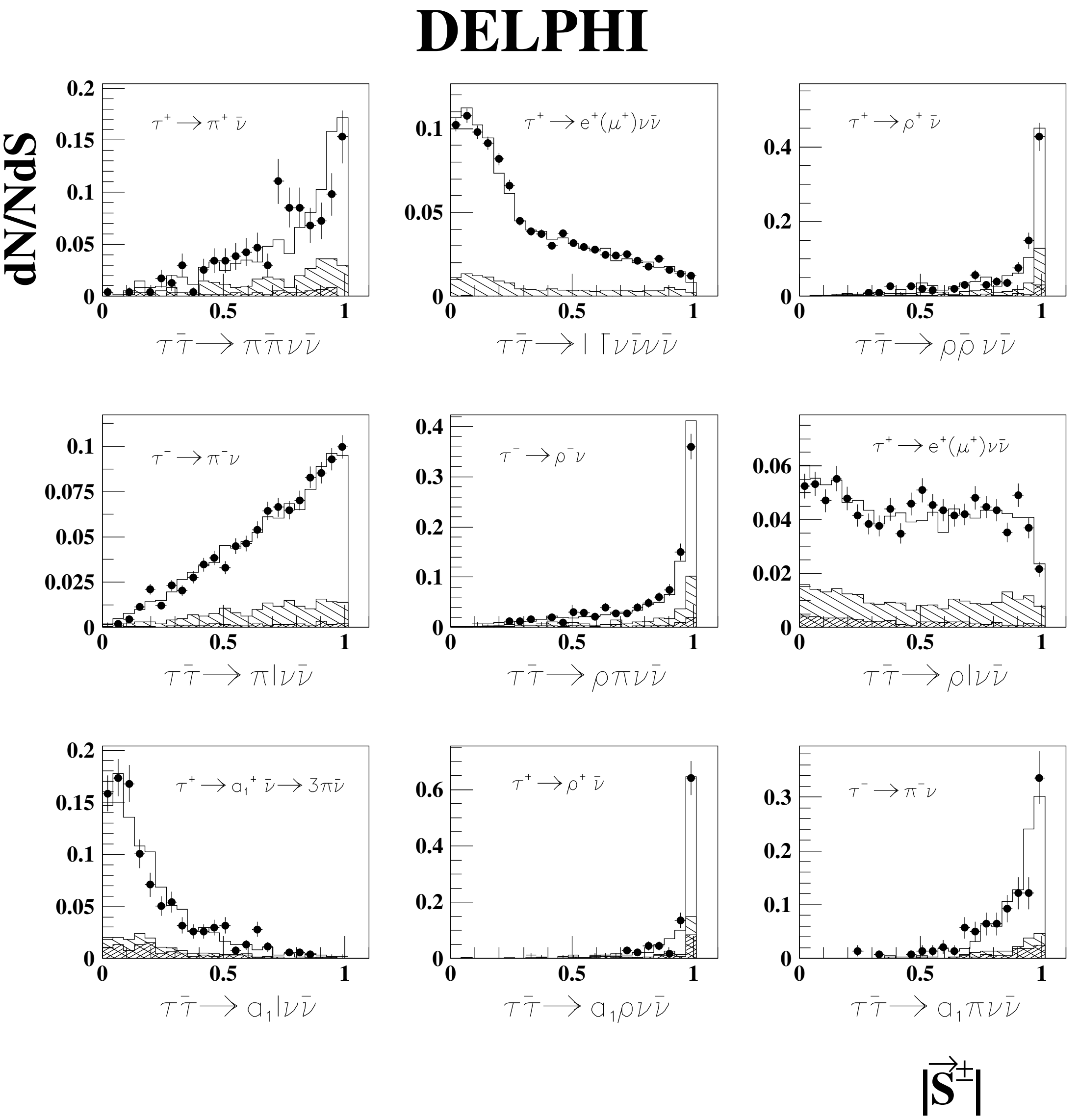

Figure 3: Distribution of the moduli of the reconstructed τ-polarisation vectors for different identified τ decay modes (indicated inside each sub-figure) in different τ-pair decay channels (indicated beneath each sub-figure). The dots with error bars show the data; the clear parts of the histograms show the simulated data; the hatched parts show the contribution of the contamination between the selected τ-pair decay channels; and the double hatched parts show the background contribution from other τ-pair events as well as from non-τ events.

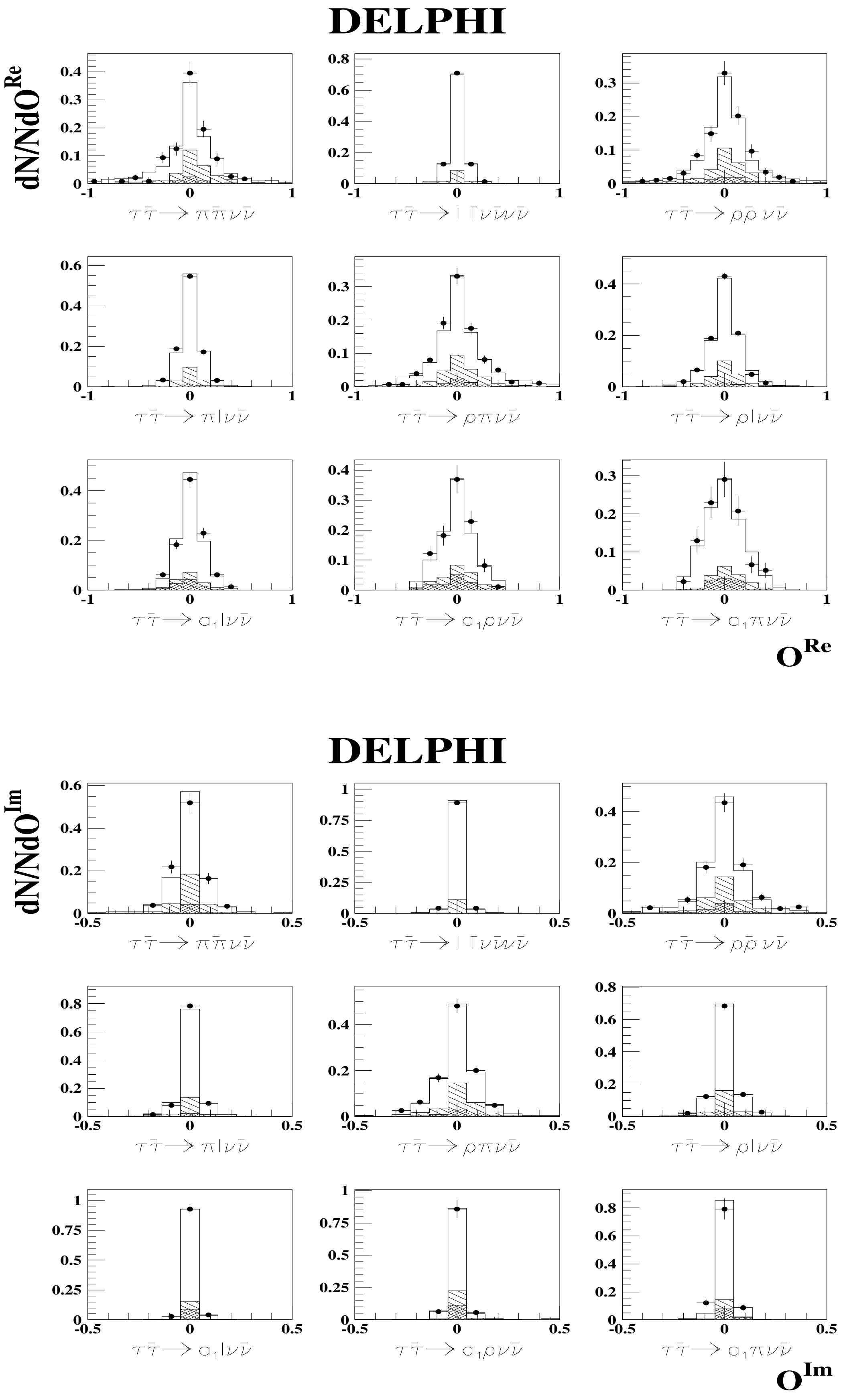

Figure 4: Distribution of the optimal CP-odd observables, $\mathcal{O}^{Re}_{Im}$, with the same graphic convention as for Fig. 3.

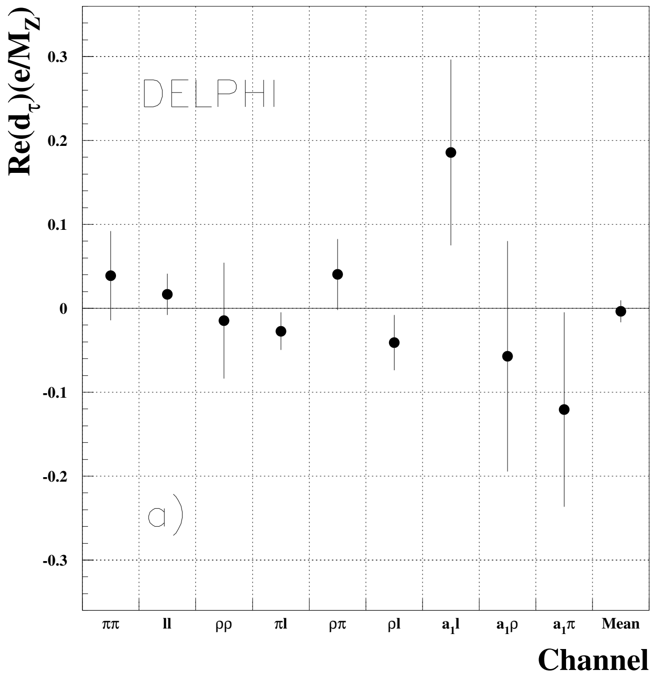

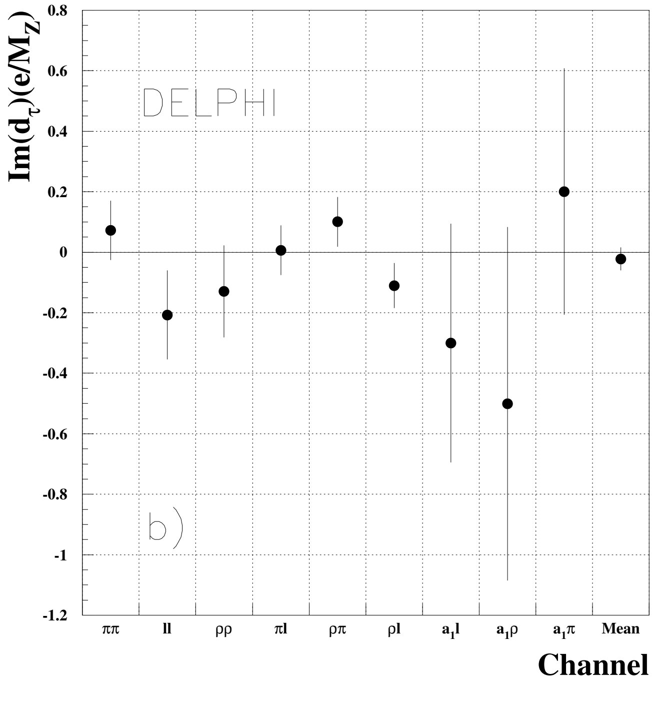

Figure 5: The measurement results of the (a) real and (b) imaginary part of the weak dipole moment, $\mathrm{Re}(d_\tau^w)$ and $\mathrm{Im}(d_\tau^w)$. The means (on the right) are the weighted average values over all the channels.